

유도전동기 베어링고장진단을 위한 고정자전류프로세싱 기술개발

(Stator Current Processing Based Technique for Induction Motors Bearing Faults Diagnosis)

홍원표, 윤충섭, 김동화

(Won-Pyo Hong · Sup-Chung Yoon, Dong-Hwa Kim)

요 약

이 논문은 다른 종류의 유도전동기 구름베어링 손상을 유도전동기 고정자 전류신호해석을 통하여 검출하고 실시간으로 손상을 진단하는 알고리즘을 개발하였다. 유도전동기 구름베어링의 손상을 검출하기 위하여 정상적인 베어링을 갖는 유도전동기, 축정열에 불량을 가지고 있는 전동기와 베어링 외륜에 구멍을 가지고 있는 2가지 종류의 비정상 베어링을 갖는 유도전동기 3set를 실험시스템을 구축하였다. 또한 유도전동기의 구름베어링시스템의 비정상적인 상태에서 고정자전류를 검출하기 위하여 TMS320F2407 DSP 칩을 이용하여 데이터 획득보드를 개발하였다. 이 고정자전류신호를 해석을 통하여 베어링 손상을 검출하기 위한 방법으로 FFT, 웨이브렛 분석 및 내적에 의한 평균신호패턴에 의한 분석결과를 제시하였다. 특히 내적에 의한 신호분석을 통하여 베어링 손상 여부를 실시간으로 진단할 수 있는 새로운 알고리즘과 분석방법을 제시하였다

1. Introduction

It is well known that induction motors dominate the field of electromechanical energy conversion. These machines find a wide role in most industries in particular in the electric utility industry as auxiliary drives in central power plants of power system, as well as a restrictive role in low MVA power supply systems as induction generators, mining industries, petrochemical industries, as well as aerospace and military equipment. Therefore, assessment of the running conditions and reliability of these drive systems is crucial to avoid unexpected and catastrophic failures. Consequently, the issue of the preventive maintenance and noninvasive diagnosis of the condition of the induction motor drives is of great concern, and is becoming increasingly important [1-3]. Motor reliability studies [4] specifically apply to machine, 100Hp or more, that are operated in industrial and commercial installations. The results of these studies show that bearing problems account for over 40% of all machine failures. Over the past several decades, rolling-element (ball or roller) bearings have been utilized in many electric machines while sleeve (fluid film) bearings are installed in only the largest industrial machines. In the case of induction motors, rolling element bearings are overwhelmingly used to provide rotor support. Lubricant contamination and lubricant loss are the most common causes of bearing failures[5]. Other common causes of bearing failures include excessive loading, corrosive environments, and misapplication.

Most of these failures start small then propagate or expand, causing the whole machine to breakdown eventually. Vibration monitoring is a reliable tool for bearing failures. The vibration data typically contain fault signatures and salient fault features because of direct measurement of the critical signal and placement of the vibration sensor[6]. However, placing a sensing device on the motor might not be possible or practical in many applications, especially for a facility that employs a large number of electric machines. The stator current, on the other hand, is readily available in many applications, and is usually measured for motor protection. Therefore, current-based fault detection has become an attractive area for bearing condition monitoring. The main disadvantage of using the current for bearing condition monitoring is the difficulty of distinguishing bearing fault signatures from non-fault components or noise in the stator current. Fault detection based on motor current relies on interpretation of frequency components in the current spectrum that are related to rotor or bearing. However, the current spectrum is influenced by many factors, including electric supply, static, and dynamic load conditions, noise, motor geometry, and fault conditions. This condition may lead to errors in fault detection. We have focused our research on so called motor current signature analysis. To carry out this research, therefore, this paper takes the initial step of investigating the efficacy of current monitoring for bearing fault detection by incipient bearing failure[7,8]. Our group has developed the embedded distributed fault tolerant and fault diagnosis system for industrial motor. These mechanisms are

based on two 32-bit DSPs and each TMS320F2407 DSP module is checking stator current, voltage, temperatures, vibration and speed of the motor. The DSPs share information from each sensor or DSP through DPRAM with hardware implemented semaphore. And it communicates the motor status through field bus (CAN, RS485). We set the experimental test bed to detect the rolling element bearing misalignment of 3 type induction motors with normal condition bearing system, shaft deflection system by external force and a hole drilled through the outer race of the shaft end bearing of the four pole test motor. The failure modes are reviewed and the characteristics of bearing frequency associated with the physical construction of the bearings are defined. The effects on the stator current spectrum are described and related frequencies are also determined. This is an important result in the formulation of a fault detection scheme that monitors the stator currents. We utilized the FFT and Wavelet analysis and averaging signal pattern tool to analyze stator current components.

2. Bearing Fault Causes

Rolling-element bearings generally consist of two rings, an inner and outer, between which a set of balls and rollers rotate in raceways. Under normal operating conditions of balancing load and good alignment, fatigue failure begins with small fissures, located below the surfaces of the raceway and rolling elements, which gradually propagate to the surface generating detectable vibrations and increasing noise level[5]. Continued stressing cause fragments of the material to break loose producing the localized fatigue phenomena known as flaking or spalling. Bearing faults can generally be grouped into two categories: single-point defects and generalized roughness. Single point defects are visible defects that appear on the raceways, rolling element, or cage, and produce specific frequency components in machine vibration, known characteristic fault frequencies. Once started, the affected area expands rapidly contaminating the lubrication and causing localized overloading over the entire circumference of the raceway. These predictable frequency components typically appear in machine vibration and are often reflected into the state current. Failure modes that cause such defects include appalling, brinelling, electric discharge machining, and corrosion [5]. The other group of bearing faults, generalized roughness, refers to an unhealthy bearing whose damage is not apparent to the invisible defects. Examples of the failure mode include deformation or warping of the rolling elements

or raceways and overall surface roughness due to heating, contaminated lubricant, or electric discharge machine. The effects produced by this failure mode are difficult to predict, and there are no characteristic fault frequency for the current or vibration associated with this type of fault. Nevertheless, they alter the vibration and state current spectra of the machine in some measurable fashion. This type of failure would usually cause RMS value of the machine vibration to increase, in a noticeable manner over a broadband. When a ball is defective, or when it rolls over a defective raceway, it produces an impact against the raceway and generates a detectable and sound pulse. The frequencies at which these pulses and vibrations occur are predictable and depend on which surface of the bearing contains the fault. The frequencies also depend on the geometrical dimensions of the bearings and the rotational speed of the rotor. Therefore, there is one predictable characteristic fault frequency for each of the four parts of a given bearing, running at a certain rotor speed in Hertz, F_R . These fault frequencies are given by [6]

Cage fault: $FCF =$

$$\frac{1}{2} F_R \left[1 - \frac{D_B \cos \theta}{D_P} \right] \quad (1)$$

Outer raceway fault:

$$F_{ORF} = \frac{N_B}{2} F_R \left[1 - \frac{D_B \cos \theta}{D_P} \right] \quad (2)$$

Inner raceway fault:

$$F_{IRF} = \frac{N_B}{2} F_R \left[1 + \frac{D_B \cos \theta}{D_P} \right] \quad (3)$$

Ball fault:

$$F_{BF} = \frac{D_P}{2D_B} F_R \left[1 - \frac{D_B^2 \cos^2(\theta)}{D_P^2} \right] \quad (4)$$

Where N_B is the number of balls, D_B is the ball diameter, D_P is the ball pitch diameter, and θ is the ball contact angle (typically equal 00). For simplicity, f_i and f_o are used in this paper for the fault frequencies related to inner race and outer race defects, respectively. The four characteristic fault frequencies are defined in (1)-(4) and illustrated in Fig. 1. The majority of bearing condition monitoring schemes focus on the detection of the characteristic fault frequencies because of the ability to discriminate

between different types of faults and correlate between change in amplitude and fault severity. The main disadvantage of depending only on detecting the fault frequencies is that these frequency components may not be useful for detecting incipient faults. Typically, absolute vibrations or motions of the electric machine do not get reflected in the stator current. There are many sources of machine vibration that can also disturb in the air-gap. A bearing single point defect produces a relative, radial motion between the stator and rotor of the machine, and this mechanical displacement affects the current spectrum in a manner similar to an air gap eccentricity. The characteristic fault frequencies are essentially modulated by the electrical supply frequency, and the resulting fault frequency components in the stator current are predicted by

$$f_{bng} = |f_e \pm m \cdot f_v| \quad (5)$$

Where f_e is the electrical supply frequency, $m=1,2,3,\dots$ and f_v is one of the four characteristic vibration fault frequencies defined by (1) through (4).

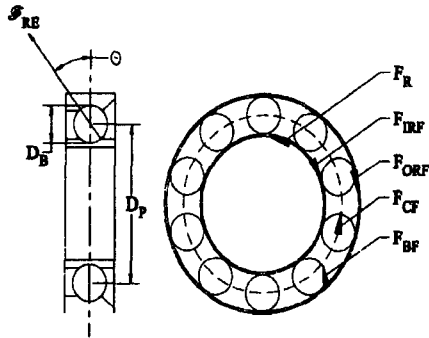


Fig.1 Dimensions and frequencies related to the characteristic fault frequency

3. Stator Current Signature Analysis

The relationship of the bearing vibration to the stator current spectrum can be determined by remembering that any air gap eccentricity produces anomalies in air gap flux density [7]. In the case of a dynamic eccentricity that varies with rotor position, the oscillation in the air gap length cause variations in the air flux density. This, in turn, affects the inductances of the machine producing stator current harmonics with frequencies predicted by

$$f_{ecc} = f_e \left[1 \pm k \left(\frac{1-s}{\frac{p}{2}} \right) \right] = |f_e \pm k \cdot F_R| \quad (6)$$

Where f_e is the electrical supply frequency, $k = 1, 2, 3, \dots$, s is the per unit slip, p is the number of machine poles, and F_R is the mechanical rotor speed in Hertz. Since ball bearing support the rotor, any bearing defect will produce a radial motion between the rotor and the stator of the machine. The mechanical displacement resulting from the damaged bearing causes the air gap of the machine to vary in a manner that can be described by a combination of rotating eccentricities moving in both directions, i.e., clockwise and counterclockwise. As with the air gap eccentricity, these variations generate stator currents at predictable frequencies,

f_{bng} , related to the vibration, electrical supply frequencies and the bearing dimensions shown in Fig. 1. They are given by the formula (5) [8].

In radially loaded bearings, the contact areas of the balls and raceways carry the heaviest loads causing most fatigue failures to involve these components. The ball spin frequency is caused by the rotation of each ball about its center. Since a defect on a ball will contact with both the inner and outer races during every revolution, the ball defect frequency is twice the spin frequency and can be written as the formula (4). The outer and inner raceway frequencies are produced when each ball passes over a defect. This occurs n -times during a complete circuit of the raceway where N_B is the number of balls. This causes the outer and inner raceway frequencies to be defined as (2) and (3), respectively. Bearing cage faults generally bind the balls producing skidding and slipping along the raceway. These effects cause high frequency vibrations to be generated. It should be noted from (2) and (3) that specific information concerning the bearing construction is required to calculate the exact characteristic frequencies. However, these characteristic race frequencies can be approximated for the most bearings with between six and twelve ball by [9].

$$f_o = 0.4 N_B \cdot f_{rm} ;$$

$$f_i = 0.6 N_B \cdot f_{rm} \quad (7)$$

This generalization allows for the definition of frequency bands where the bearing race frequencies

are likely to show up without requiring explicit knowledge of the bearing construction. Therefore, it is possible to formulate an effective fault detection scheme, which monitors the related stator current spectrum for bearing defects.

4. Stator Current Monitoring system

The stator current monitoring system contains the four processing section illustrated in Fig. 2.

A. Sampler

The purpose of the sampler is to monitor a single phase of induction motor current. This is accomplished by removing the 60-Hz excitation component through low-pass filtering and sampling the resulting signal. The current flowing in single phase of the induction motor is sensed by a current transformer and sent to a 60 Hz notch filter, where the fundamental component is reduced. The analog signal is then amplified and low-pass filtered. The filtering removes the undesirable high frequency components that produce aliasing of the sampled signal while the amplification maximizes the use of the analog-digital (A/D) converter input range.

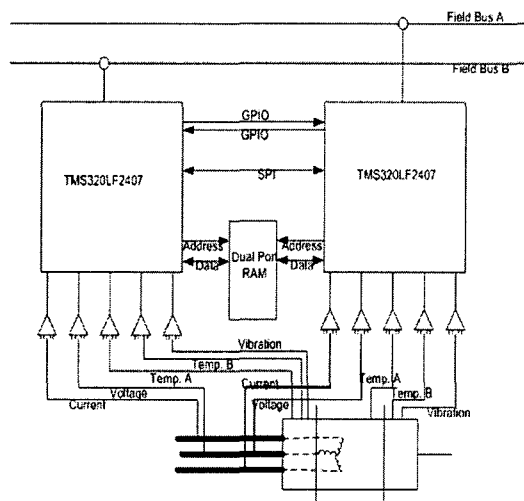


Fig.2 Block diagram of single-phase stator current monitoring Scheme

The A/D converter samples the filtered current signal at a predetermined sampling rate that is an integer multiple of 60Hz. This is continued over a sampling period that is sufficient to achieve the required fast Fourier transform (FFT).

B. Preprocessor

The preprocessor converts the sampled signal to frequency domain using an FFT algorithm. The

spectrum generated by this transformation includes only the magnitude information about each frequency component. Averaging a predetermined number of generated spectra reduces signal noise that is present in the calculated spectrum. This can be accomplished by using either spectra, calculated from multiple sample sets or spectra computed from multiple predetermined sections (or windows) of a single large sample set. Because of the frequency range of interest and the desired frequency resolution, the processing section generates several thousand-frequency components.

C. Fault detection algorithm

In order to reduce the large amount of spectral information to a usable level, an algorithm, in fact frequency filter eliminates those components that provide no useful failure information. The algorithm keeps only those components that are of particular interest because they specify characteristic frequencies in the current spectrum that are known to be coupled to particular motor faults. Since the slip is not constant during normal operation, some of these components are bands in the spectrum where the width is determined by the maximum variation in the slip of the motor. We installed the vibration sensor, the stator thermal sensor, supply voltage sensor including stator current sensor. Continual studies are carried out to find the fault detection algorithm of induction motors.

D Monitoring system

The monitoring system diagnostics the frequency components and then classifies them for the various type faults of induction motor. This provides the important decision information for the faults of induction motors.

5. Experimental results

For this method, the stator current monitoring system is sketched in Fig. 3. Modern measurement techniques in combination advanced computerized data processing and acquisition show new ways in the field induction machines monitoring by the use of spectral analysis of operational process parameters. Time domain analysis using characteristic values to determine changes by trend setting, spectrum analysis to determine trends of frequencies, amplitude and phase relations, as well as spectrum analysis to detect periodical components of spectra are used as evaluation tools. To verify the generality of the presented considerations laboratory experiments were performed with three induction motors. The low pass filter with 2kHz cutoff frequency was used to eliminate the high frequency region. The stator current was sampled with a 4-KHz sampling rate and interfaced to an embedded distributed fault tolerant and fault diagnosis system for industrial

motor. These mechanisms are based on two 32-bit DSPs and each TMS320F2407 DSP module is checking stator current, voltage, temperatures, vibration and speed of the motor. The DSPs share information from each sensor or DSP through DPRAM with hardware implemented semaphore. And it can communicate motor status through field bus (CAN, RS485). And, then the DSP data acquisition system is connected to the Pentium PC. We set the experimental test bed to detect the rolling element bearing misalignment of 3 type induction motors with normal condition bearing system, shaft deflection system by external force and a hole drilled through the outer race of the shaft end bearing of the four pole test motor.

A. Fault detection technique 1

The first experiment involved the drive system driving at 1000 rpm. Time domain analysis of the stator current is shown in Fig. 5. They depict the time domain analysis results of the supposed normal condition bearing system, a hole drilled through the outer race of the shaft end bearing and shaft deflection system by external force of the four pole test motor, respectively. The experimental results show a uniform pattern with the peak to peak interval, and the magnitudes of pattern of bearings with a hole drilled through the outer raceway and shaft deflection by external force have the higher values than that of the normal bearing system.

B. Fault detection technique 2(FFT: Fast Fourier Transform)[9,10]

Generally, induction motor fault detection via FFT-based stator current signature analysis could be improved by decreasing the current waveform distortions as is illustrated by Fig. 6. Moreover, it is

well known that motor current is a non-stationary signal,

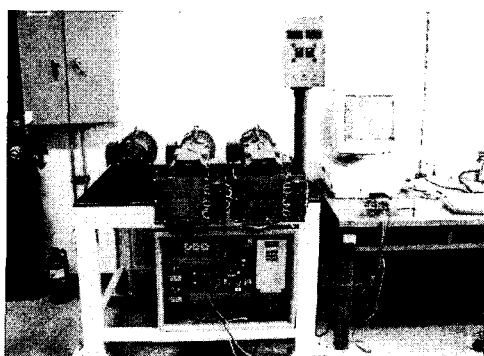


Fig.3 View of the experimental setup

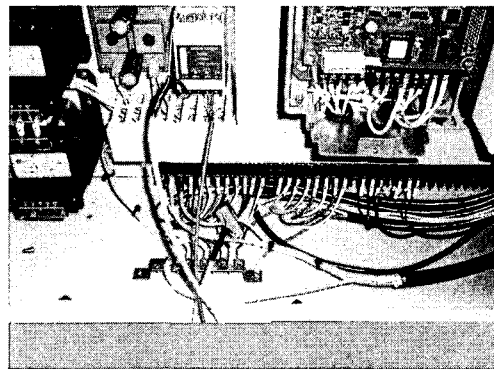


Fig. 4 Sensing part of stator single-phase current of induction motors

the properties of which vary with the time varying normal operating conditions of the motor. As a result, it is difficult to differentiate fault conditions from the normal operating conditions of the motor using Fourier analysis. The maximum frequency of horizontal line in Fig. 6 is 1000Hz. This figures show that the current spectrum of less than 500Hz is dominant.

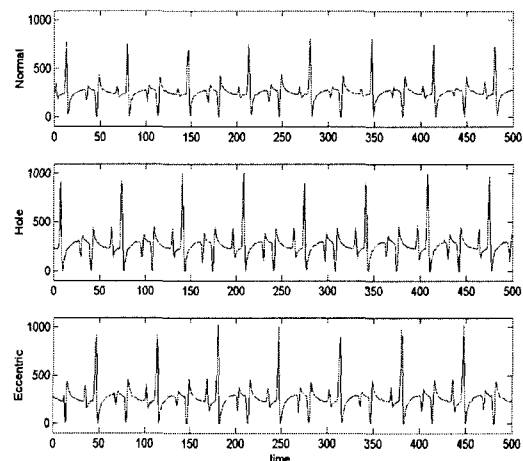


Fig. 5 Time domain analysis of stator current signature

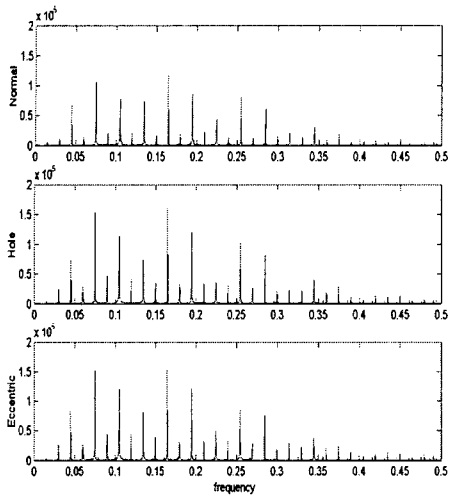


Fig. 6 Stator current power spectra of health, hole and shaft deflection motor

C. Fault detection technique 3 (Wavelet analysis)[11]

Wavelets are a recently developed mathematical tool for signal analysis. Informally, a wavelet is short-term duration wave. Wavelets are used as a kernel function in an integral transform, much in the same way that sines and cosines are used in Fourier analysis. The main advantage of Wavelets analysis over Fourier analysis is that it does not require time function involved to be periodic. This means that wavelet could be applied for the transient analysis and faults detection because, in this case, the stator current is generally not a periodic function of time. The wavelet technique can be used for a localized analysis in the time-frequency or time scale domain.

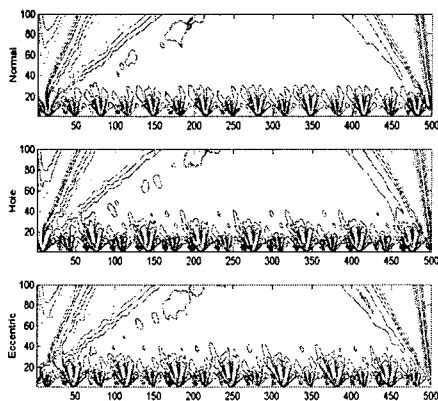


Fig. 7 Wavelet map of motor current signature

Fig. 7 shows the result of stator current spectrum by continuous Wavelet transform. Fig. 8 is alternately represented by scale factor of Fig 7 as following

$$W(a) = \sum_{n=1}^N |W^f(a, n)|^2 \quad (8)$$

where N is the number of collected signal, a is a scale factor and $W^f(a, n)$ is the result of continuous wavelet transform.

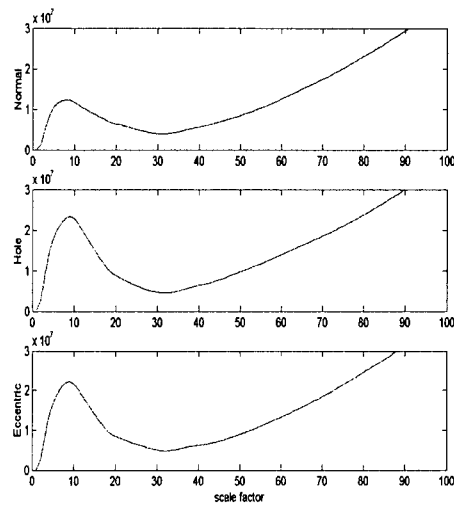


Fig. 8 Energy distribution by scale factor

Under the not sever situation of the bearing faults, It is also difficult to differentiate fault conditions from the normal operating conditions of the motor using Wavelet analysis, even if we see a little difference low scale factor (from 0 to 30).

D. Fault detection technique 4 (Inner product of wave patterns)

From Fig. 1, it shows a repeatable signal pattern for 3 case motors. This signal repetition consists of 63 data from peak to peak. An average signal pattern for corresponding points of 10's by arbitrarily choosing is described at Fig. 9.

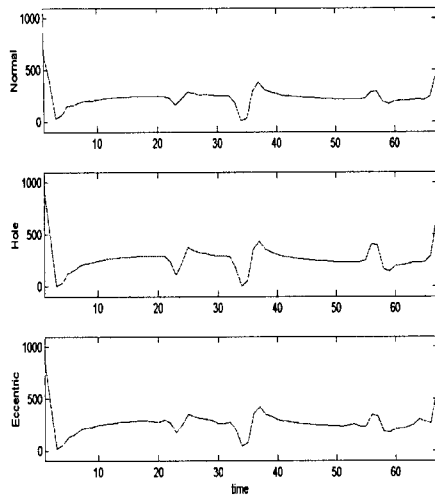


Fig. 9 Averaged signal pattern

The normalized inner production of two different patterns is given by

$$IP_n = \left(\sum_{i=1}^N a_i \cdot b_i \right) / IP_{normal} \quad (9)$$

Where, IP_{normal} is the inner product of normal patterns and $a_i, b_i (i = 1, \dots, 63)$ are the temporary data elements of each pattern.

Table 1. Normalized inner product

	Normal	Hole	Eccentric
1	1.1133	1.1805	1.1998
2	1.1000	1.1997	1.1956
3	1.1112	1.1767	1.1868
4	1.1100	1.1801	1.1990
5	1.1138	1.1770	1.1918
6	1.1064	1.1699	1.1851
7	1.1231	1.1895	1.2036
8	1.1155	1.1973	1.1873
9	1.0967	1.1934	0.9443
10	1.1205	1.1954	1.1712

The result of Equation 9 shows in the table 1. The numerical values of the holed and eccentric bearing are higher than that of normal condition bearing except 9th eccentric case. Also it shows the eccentric case is a little higher than holed case. The proposed inner product of pattern is not required a mass calculation time like FFT, Wavelet and others. So, it is suitable to MPU or DSP in sense of less computation and memory space requirement.

We can improve the reliability by comparing different patterns which are stored on MPU/DSP.

VI. Conclusions

We have focused our research on so called motor current signature analysis. To carry out this research, therefore, this paper takes the initial step of investigating the efficacy of current monitoring for bearing fault detection by incipient bearing failure. Our group has developed the embedded distributed fault tolerant and fault diagnosis system for industrial motor. These mechanisms are based on two 32-bit DSPs and each TMS320F2407 DSP module is checking stator current, voltage, temperatures, vibration and speed of the motor. The DSPs share information from each sensor or DSP through DPRAM with hardware implemented semaphore. And it communicates the motor status through field bus (CAN, RS485). We set the experimental test bed to detect the rolling element bearing misalignment of 3 type induction motors with normal condition bearing system, shaft deflection system by external force and a hole drilled through the outer race of the shaft end bearing of the four pole test motor. The failure modes are reviewed and the characteristics of bearing frequency associated with the physical construction of the bearings are defined. The effects on the stator current spectrum are described and related frequencies are also determined. This is an important result in the formulation of a fault detection scheme that monitors the stator currents. We utilized the FFT, Wavelet analysis and averaging signal pattern tool to analyze stator current components.

Appendix

Rated parameters of the machine under test

Power	1.5	kW
Frequency	60	Hz
Voltage(Δ/Y)	220/380	Volt
Current(Δ/Y)	3	Ampere
Speed	1800	rpm
Pole pairs	2	pair

Acknowledgment

The authors would like to gratefully acknowledge the financial support of KESRI (Korea Electrical Engineering & Science Research Institute) and ETEP of KEPRI under the project number A3050.

References

- [1] O.V. Thorsen et al., "A survey of faults on induction motor in offshore oil industry, petrochemical industry, gas terminals, and oil refineries", IEEE Trans. Industry application, Vol. 31, pp. 1186-1196, Sept./Oct., 1995.
- [2] M.E.H. Benbouzid, "Bibliography on induction faults detection and diagnosis", IEEE Trans. Energy Conversion, Vol. 14, No. 4, pp. 1065-1074, DEC., 1999.
- [3] M.E.H. Benbouzid et al., "What stator current processing-based technique to use induction motor rotor faults diagnosis", IEEE Trans. Energy Conversion, Vol. 18, No. 2, June 2003.
- [4] IAS Motor Reliability Working Group, "Report of large motor reliability survey of industrial and commercial installations: Part I", IEEE Trans. Industrial Application, Vol. 21, No. 4, pp. 853-864, July 1985.
- [5] P. Eschman et al., "Ball and Roller bearings: Their Theory, Design, and Application", K.G Heyden, 1958.
- [6] R. A. Collacott, "Vibration Monitoring and Diagnosis", John Wiley & Sons, pp. 109-111, 1979.
- [7] R. R. Shoen et al., "Effect of time varying load on rotor fault detection in induction machines", in Conf. Rec. 28th Annual IAS Meeting, Oct. 1993, pp324-330.
- [8] R.R Shoen et al., "Motor bearing damage detection using stator current monitoring", IEEE Trans., Ind. Application, Vol. 31, pp. 1274-1279, Nov./Dec. 1995.
- [9] R. L. Schiltz, "Forcing frequency identification of rolling element bearing", Sound and Vibration, pp. 16-19, May 1990.
- [10] L. Cohen, "Time frequency Analysis", Prentice-Hall, 1995.
- [11] S.H Lee et al., "Introduction to the Wavelet Transform, Jinhua Book Inc., 2002.